Available online at www.sciencedirect.com
ScienceDirect
Journal of Power Sources 171 (2007) 670–677
JOURNAL OF POWER SOURCES
www.elsevier.com/locate/jpowsour

Diagnosis of PEM fuel cells through current interruption

M.A. Rubio *, A. Urquia, S. Dormido

Departamento de Informática y Automática, UNED, Juan del Rosal 16, 28040 Madrid, Spain

Received 24 January 2007; received in revised form 25 May 2007; accepted 17 June 2007
Available online 23 June 2007

Abstract

A novel methodology for the on-line diagnosis of PEMFC, intended to be used in portable control systems, is proposed. First, an equivalent-circuit model for PEMFC is proposed. This model has a low computational cost and it allows reproducing the dynamic behavior of the PEMFC. The relationship among the parameters of this simplified model and PEMFC electrochemical parameters is stated. Secondly, a procedure to estimate all the parameters of this model from the cell's transient response after current interruption (CI) is proposed. The equipment required to make these CI measurements is easily portable and inexpensive. Thirdly, the procedure to calculate some relevant PEMFC electrochemical parameters from the equivalent-circuit parameters is discussed. These PEMFC parameters are the double layer capacitance, the diffusion resistance, the charge transfer resistance, the diffusion-related time constant, and the membrane resistance. Finally, this PEMFC assessment methodology is applied to the diagnosis of the cathode flooding. The diffusion resistance is found to have a dominant effect on the amount of water accumulated inside the cell. The described methodology can be used to characterize other phenomena, including the cathode and membrane drying, the membrane degradation, and the anode poisoning by carbon monoxide.

Keywords: Diagnosis; Current interruption; Flooding; Impedance spectroscopy

1. Introduction

Our society is suffering from fossil fuel shortage. Fossil fuels (i.e., coal, oil, and natural gas) also contribute to a number of environmental problems during their extraction, transportation, and use. In particular, their use to obtain energy generates emissions that contribute to global warming and climate change. As an alternative, fuel cells are one of the most promising means of producing energy in portable systems.

A considerable research effort has been made in order to understand the physical and chemical phenomena involved in the PEMFC operation. Numerous mathematical models have been proposed, including 1D [1–4], 2D [5], and 3D [6,7] static models; and 1D [8,9], and 3D [10] dynamic models. The water flooding in the PEMFC cathode has been modelled from physical–chemical first principles [11]. These detailed models contain a large number of adjustable parameters and their computation time is large. As a consequence, these models are not well suited for control applications.

PEMFC models with low computational cost, intended for use in control applications, have also been developed. Randles electric models are frequently used in this context. The combined use of EIS and Randles models for over-potential calculation was proposed by Wagner [12]. The anode poisoning by carbon monoxide was discussed by Ciureanu and Wang [13]. The relationship between the amount of water and the cell resistance was studied by Andreaus et al. [14], and Yuan et al. [15]. The effect of the cathode flooding and drying on the cell behavior was addressed in [16].

In this context, EIS techniques are employed to study the fuel cell behavior, and to estimate the value of the cell model parameters [17–20]. However, EIS equipment is too expensive and bulky for use on in-field assessment of operating commercial cells. As a consequence, this approach to PEMFC diagnosis is not suited for in-field control applications.

An alternative methodology for the in-field diagnosis of PEMFC, that can be implemented in portable control systems, is proposed in this manuscript. To achieve this goal, a Randles electric model of the PEMFC is proposed. This dynamic model has a low computational cost and it has been specially formulated to facilitate the estimation of their parameters from the cell response after current interruption (CI). The advantage of

* Corresponding author. Tel.: +34 913987147; fax: +34 913987690.
E-mail addresses: marubio@dia.uned.es (M.A. Rubio), aurquia@dia.uned.es (A. Urquia), sdormido@dia.uned.es (S. Dormido).

0378-7753/$ – see front matter © 2007 Elsevier B.V. All rights reserved.
doi:10.1016/j.jpowsour.2007.06.072

Nomenclature

C_{dl}	double layer capacitance (F)
C_e	number of electrons in 1 C (C^{-1})
C_g	concentration in cathode active layer (mol m^{-3})
D	diffusion coefficient (m^2 s^{-1})
E_{oc}	open-circuit voltage (V)
F	Faraday constant (F)
j	imaginary unit
M_{H_2O}	water molar weight (18.0157 g mol^{-1})
n	number of electrons
N_A	Avogadro constant (6.0221415 mol^{-1})
R	perfect gas constant (J mol^{-1} K^{-1})
R_d	diffusion resistance (Ω)
R_m	membrane resistance (Ω)
R_p	charge transfer resistance (Ω)
s	laplace transform variable
S	active area (m^2)
S_a	electrode surface (cm^2)
T	temperature (K)
Z_W	Warburg

Greek letters

δ	diffusion layer width (m)
η_a	anode over-voltage (V)
η_c	cathode over-voltage (V)
η_m	membrane over-voltage (V)
τ_d	diffusion-related time constant (s)
χ_{H_2O}	water load (g cm^{-2})
ω	frequency (rad s^{-1})

this approach is that the equipment required to perform the CI experiments is inexpensive and easily portable.

The relationship among the parameters of this Randles model and the following PEMFC electrochemical parameters is discussed: the double layer capacitance, the diffusion resistance, the charge transfer resistance, the diffusion-related time constant, and the membrane resistance. The procedure to estimate the value of these physical parameters from the Randles model parameters is proposed.

The use of CI techniques for cell state characterization is not new. Some cell diagnosis methods, based on the CI technique, have been proposed by other authors. In particular, CI techniques can be successfully applied to the estimation of the FC resistance [21]. Other methods, based on the analysis of the cell response after a step change in the load, are used to validate the data obtained from the EIS study [22].

As a difference with other authors' methods, the proposed methodology allows estimating the significant operation parameters of the PEMFC only from the CI data. Rich information about the cell dynamic behavior is contained in the cell response to step and impulse inputs. In this case, the information is extracted from the cell response after CI. The impulse has a wide spectrum of frequencies, exciting the FC fundamental phenomena [23–25].

2. Experimental set-up and procedure

In order to study the effect of the cathode flooding on the cell model parameters, the parameter estimation methodology proposed in Section 3 is repeatedly applied during the flooding process. The data obtained from each CI experiment run, corresponding to a given cathode flooding level, is used to estimate the parameters of the cell electric model. The experiment results are discussed in Section 4.

2.1. Experimental set-up

PEMFC characteristics: 25 cm^2 electrode surface; NAFION 112 membrane; electrodes of coal cloth; and double serpentine topology in anode and cathode. *Initial experimental conditions*: 26 °C and 60% relative humidity. *Experimental conditions*: cell temperature is not controlled.

2.2. Experimental procedure

The PEMFC is fed with hydrogen and oxygen at the same pressure: 0.5 bar. The anode and cathode exhausts are kept closed. An electric load of 0.066 Ω is connected. Periodically, CI are performed and an oscilloscope (Tektronix THS720) is used for cell voltage reading (2500 readings per CI test), with a sample period of 2 ms.

In order to study the effect of the cathode flooding on the cell voltage and current, a data-acquisition card (PCLab PCL812G) and LabVIEW are used to record the cell voltage, with a sample period of 1 s. This experimental data is used to estimate the amount of water produced in the electrochemical reaction (as it is discussed in Section 3.8).

2.3. Uncertainty analysis

- *Tektronix THS720 oscilloscope*: dc voltage range, 400.0 mV to 880 V; dc volts accuracy, ± (0.5% of reading + 5 counts).
- *PCLab PCL812G card*: its measurement accuracy is ±0.015% of the complete range.
- *Electric load*: it was calibrated using the HP 4192A impedance analyzer, which has a measurement error of ±0.1%.

3. Analysis and modelling

3.1. Main assumptions

The voltage drop across the fuel cell (V_{cell}) can be written as a function of the steady-state open-circuit voltage of the cell (E_{oc}), and the over-voltages of the anode (η_a), the cathode (η_c) and the membrane (η_m) [21,26]:

$$V_{cell} = E_{oc} - \eta_a - \eta_m - \eta_c \quad (1)$$

The open-circuit voltage (E_{oc}) is modelled as an ideal voltage source. The external operating conditions are kept constant during the experiments. Therefore, the over-voltages (η_a, η_m, η_c)

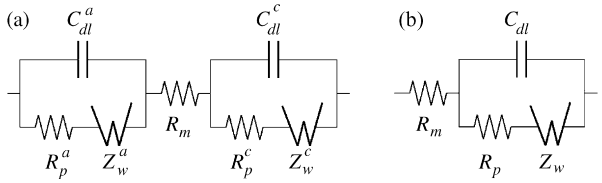

Fig. 1. PEMFC electric models: (a) complete model and (b) simplified model.

are assumed to be only dependent of the FC internal phenomena. The over-voltages of the different layers can be modelled as electric components that represent the FC dynamic behavior.

3.2. Equivalent circuit for a PEMFC

The cell voltage in Eq. (1) can be modelled by the electric circuit shown in Fig. 1a, which is composed of Randles models connected in series [22,18]. $Z_{\mathrm{W}}^{\mathrm{a}}$ and $Z_{\mathrm{W}}^{\mathrm{c}}$ are the Warburg impedances associated to the gas diffusion in the anode and the cathode, respectively. $R_{\mathrm{p}}^{\mathrm{a}}$ and $R_{\mathrm{p}}^{\mathrm{c}}$ are the charge transfer resistances in the anode and the cathode. $C_{\mathrm{dl}}^{\mathrm{a}}$ and $C_{\mathrm{dl}}^{\mathrm{c}}$ are the double layer capacities in the anode and the cathode. Finally, R_{m} is the membrane resistance.

Two additional hypotheses are made in order to simplify the cell model shown in Fig. 1a. As a result, the simplified model shown in Fig. 1b is obtained.

(1) The oxygen reduction reaction in the cathode in very slow in comparison with the hydrogen oxidation reaction [27,28]. Therefore, the anode over-voltage is very small in comparison with the cathode over-voltage. As a consequence, the anode over-voltage contribution to the cell voltage can be neglected in the model.
(2) The double layer capacity, which is usually represented by constant-phase elements, is represented by a pure, single-frequency theoretical capacity [19,16,22,29].

3.3. Modelling of the Warburg impedance

The Warburg impedance (Z_{W}) can be written in the Laplace domain as a function of the finite length diffusion [18]:

$$Z_{\mathrm{W}}(s) = R_{\mathrm{d}} \frac{\tanh\sqrt{s\tau_{\mathrm{d}}}}{\sqrt{s\tau_{\mathrm{d}}}} \tag{2}$$

where the diffusion resistance (R_{d}) and the diffusion time constant (τ_{d}) can be calculated from the following expressions:

$$R_{\mathrm{d}} = \frac{RT\delta}{SC_{\mathrm{g}}Dn^2F^2} \tag{3}$$

$$\tau_{\mathrm{d}} = \frac{\delta^2}{D} \tag{4}$$

The following approximation of the Warburg impedance in Eq. (2) is proposed:

$$Z_{\mathrm{W}}(s) = \frac{R_1^*}{1 + R_1^* C_1^* s} + \frac{R_2^*}{1 + R_2^* C_2^* s} \tag{5}$$

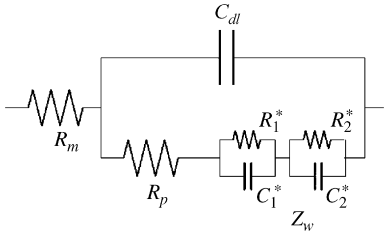

Fig. 2. PEMFC electric model with Warburg impedance calculated from Eq. (5).

Table 1
Fitted values of the parameters in Eq. (8)

Parameter	Value
R_1 (Ω)	0.8463
R_2 (Ω)	0.1033
C_1 (F)	0.3550
C_2 (F)	0.03145

where

$$R_i^* = R_i R_{\mathrm{d}} \quad \text{for } i = \{1, 2\} \tag{6}$$

$$C_i^* = C_i \frac{\tau_{\mathrm{d}}}{R_{\mathrm{d}}} \quad \text{for } i = \{1, 2\} \tag{7}$$

or, equivalently

$$Z_{\mathrm{W}}(s) = R_{\mathrm{d}} \left(\frac{R_1}{1 + R_1 C_1 \tau_{\mathrm{d}} s} + \frac{R_2}{1 + R_2 C_2 \tau_{\mathrm{d}} s} \right) \tag{8}$$

This approximation is equivalent to model the cell by using the circuit shown in Fig. 2. Four new parameters have been introduced in Eq. (8): R_1, R_2, C_1 and C_2. The values of these four parameters are calculated by fitting Eq. (8) to Eq. (2) in the frequency range from 2×10^{-1} s^{-1} to 1.5×10^{3} s^{-1}, considering $\tau_{\mathrm{d}} = 1$. The calculated values are shown in Table 1.

The exact value of the impedance, calculated from Eq. (2), and the approximated value, obtained from Eq. (8) using the previously calculated values of R_1, R_2, C_1 and C_2, are plotted in Fig. 3. Also, the absolute error is shown in Fig. 3.

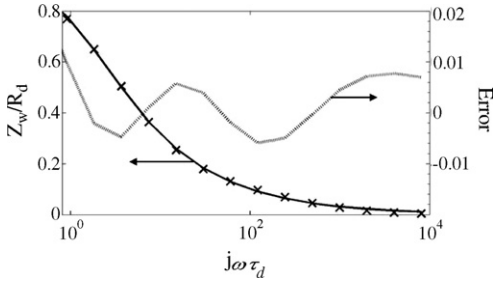

Fig. 3. Warburg impedance calculated from Eq. (2) (—) and Eq. (8) (×). Absolute error.

Table 2
Estimated parameters

Parameter	Description	Unit
C_{dl}	Double layer capacitance	F
R_d	Diffusion resistance	Ω
R_p	Charge transfer resistance	Ω
τ_d	Diffusion-related time constant	s
R_m	Membrane resistance	Ω

3.4. Modelling of the PEMFC impedance

The cell impedance (Z_{cell}), calculated from the circuit shown in Fig. 2, is the following:

$$Z_{cell}(s) = \frac{as^2 + bs + c}{ds^3 + es^2 + fs + g} \quad (9)$$

where the parameters a, b, c, d, e, f and g can be calculated from the following expressions:

$$a = 9.76 \times 10^{-4} R_p \tau_d^2 \quad (10)$$

$$b = 0.304 R_p \tau_d + 3.38 \times 10^{-2} R_d \tau_d \quad (11)$$

$$c = R_p + 0.949 R_d \quad (12)$$

$$d = 9.76 \times 10^{-4} C_{dl} R_p \tau_d^2 \quad (13)$$

$$e = 3.37 \times 10^{-2} C_{dl} R_d \tau_d + 0.3048 C_{dl} R_p \tau_d + 9.76 \times 10^{-4} \tau_d^2 \quad (14)$$

$$f = C_{dl} R_p + 0.3048 \tau_d + 0.949 C_{dl} R_d \quad (15)$$

$$g = 1 \quad (16)$$

The cell impedance described by Eq. (9) depends on the following four physical parameters: C_{dl}, R_d, R_p and τ_d. As it will be discussed later, the value of these parameters can be estimated from the cell response after CI. The estimated parameters are listed in Table 2.

3.5. PEMFC response after CI

The simplified model of the Warburg impedance proposed in Section 3.3 has been used (in Section 3.4) to obtain an analytical expression of the cell impedance. Now, this analytical expression of the cell impedance will be used to obtain an analytical expression for the PEMFC voltage response after CI.

The equivalent circuit of the CI experimental set-up is shown in Fig. 4a. The load impedance is R_{load}. The cell impedance (Z_{cell}) is calculated from Eq. (9). As the cell impedance has only real poles, the cell response after CI is equal to the cell response after a current impulse at $t = 0$ (see Section 3.7):

$$I(t) = I_0 \delta(t) \quad (17)$$

where $\delta(t)$ is the Dirac delta, and I_0 is the steady-state value of the current at $t = 0^-$. It is calculated as follows:

$$I_0 = \frac{V_{cell}(t = 0^-)}{Z_T(t = 0^-)} \quad (18)$$

where Z_T is the dc impedance of the circuit shown in Fig. 4a. The equivalent circuit of the impedance Z_T is represented in Fig. 4b.

The cell voltage can be written, in the Laplace domain, as follows:

$$V_{cell}(s) = V_{oc} - Z_{cell}(s) I(s) \quad (19)$$

The time-domain expression of the cell impedance proposed in Section 3.4 is the following:

$$L^{-1}[Z_{cell}(s)] = R_m \delta(t) + \sum_{i=1}^{3} \left(\frac{a r_i^2 + b r_i + c}{3 d r_i^2 + 2 e r_i + f} \right) e^{-r_i t} \quad (20)$$

where r_1, r_2 and r_3 are the three roots of the polynomial $ds^3 + es^2 + fs + g$.

The dynamic response of the cell voltage after CI is the following:

$$V_{cell}(t) = V_{oc} - I_0 \left(R_m \frac{1}{\sigma\sqrt{2\pi}} e^{-t^2/2\sigma^2} + \alpha_1 e^{-r_1 t} + \alpha_2 e^{-r_2 t} + \alpha_3 e^{-r_3 t} \right) \quad (21)$$

where

$$\alpha_i = \frac{a r_i^2 + b r_i + c}{3 d r_i^2 + 2 e r_i + f} \quad \text{for } i = 1, 2, 3 \quad (22)$$

and also, it must be satisfied:

$$\int_{-\infty}^{\infty} \frac{1}{\sigma\sqrt{2\pi}} e^{-t^2/2\sigma^2} \, dt = 1 \quad (23)$$

The parameter σ can be estimated from the CI experimental data as follows. The CI experimental data allow estimating the overvoltage due to the membrane resistance [30,21]. It corresponds to the abrupt rising of the voltage, from V_0 to V_s, at time $t = 0^+$ (see Fig. 5). V_0 is the initial voltage, and V_s is the voltage at $t = 0^+$. Both can be estimated from the CI experimental data. Then, the membrane resistance (R_m) can be calculated from the following expression:

$$V_s - V_0 = I_0 R_m \quad (24)$$

Finally, the dynamic response of the cell voltage can be calculated, for $t > 0^+$ (i.e., for $V_{cell} > V_s$), from the following expression:

$$V_{cell}(t) = V_{oc} - V_s - I_0(\alpha_1 e^{-r_1 t} + \alpha_2 e^{-r_2 t} + \alpha_3 e^{-r_3 t}) \quad (25)$$

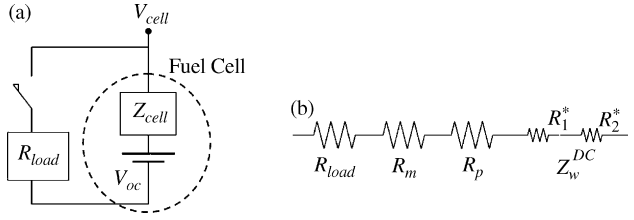

Fig. 4. CI experimental set-up: (a) equivalent circuit and (b) dc impedance (Z_T).

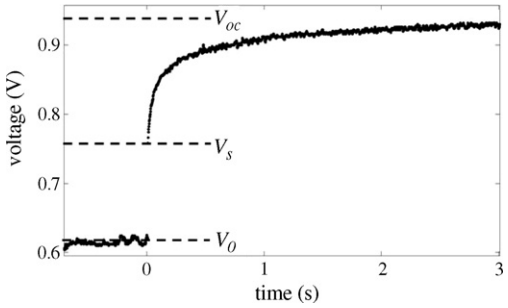

Fig. 5. Estimation of over-voltage due to membrane resistance.

where V_{oc} is the steady-state, open-circuit voltage of the PEMFC (see Fig. 5).

In order to illustrate the dynamic behavior of the simplified cell model shown in Fig. 2, the cell voltage after CI (calculated from Eq. (25)) and the impedance spectra are plotted in Fig. 6 for selected values of the parameters C_{dl}, R_d, R_p and τ_d.

3.6. Model parameter estimation from CI data

The voltage after CI of the cell represented by Eq. (9) is described by Eq. (25). The α_i coefficients depend on the roots r_i and on the parameters a, b, c, d, e and f (see Eq. (22)). These parameters depend on the physical parameters C_{dl}, R_d, R_p and τ_d (see Eqs. (10)–(15)). As a consequence, $V_{cell}(t)$ is a function of r_1, r_2, r_3, C_{dl}, R_d, R_p and τ_d.

The analytical expression of $V_{cell}(t)$ as a function of r_1, r_2, r_3, C_{dl}, R_d, R_p and τ_d is obtained by symbolic manipulation of Eqs. (25), (22), and (10)–(15). Finally, in order to estimate the value of these seven parameters (i.e., r_1, r_2, r_3, C_{dl}, R_d, R_p and τ_d), this analytical expression of $V_{cell}(t)$ can be fitted to the experimental data of the cell voltage after CI (for $V_{cell} > V_s$).

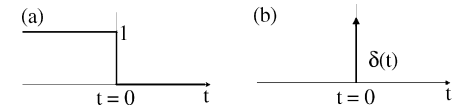

Fig. 7. Input signals: (a) interruption step and (b) unit impulse.

The procedure described in this section allows estimating the value of the parameters R_m, C_{dl}, R_d, R_p and τ_d. These parameters completely define the simplified model of the fuel cell shown in Fig. 2.

3.7. Interruption step and impulse responses

Consider a plant transfer function described by Eq. (26). It will be demonstrated that the plant response to the following two input signals is the same: an interruption step and a unit impulse (see Fig. 7):

$$F(s) = \sum_i \frac{k_i}{1 + k_i \tau_i s} \quad \text{where } k_i, \tau_i \in \Re \text{ and } k_i, \tau_i > 0 \tag{26}$$

The plant response to the interruption step can be calculated by subtracting the response to a unit step, $u(t)$, from that to $f(t) = 1$ (i.e., the interruption step can be written as $1 - u(t)$).

The plant response to a unit step is the following:

$$L^{-1}\left[F(s)\frac{1}{s}\right] = L^{-1}\left[\sum_i \frac{k_i}{s(1 + k_i\tau_i s)}\right] = \sum_i k_i(1 - e^{-t/k_i\tau_i}) \tag{27}$$

The plant response to $f(t) = 1$ is equal to the plant steady-state response to a unit step:

$$\lim_{t\to\infty}\left\{L^{-1}\left[F(s)\frac{1}{s}\right]\right\} = \lim_{s\to 0}\left\{sF(s)\frac{1}{s}\right\} = \lim_{s\to 0}\{F(s)\} = \sum_i k_i \tag{28}$$

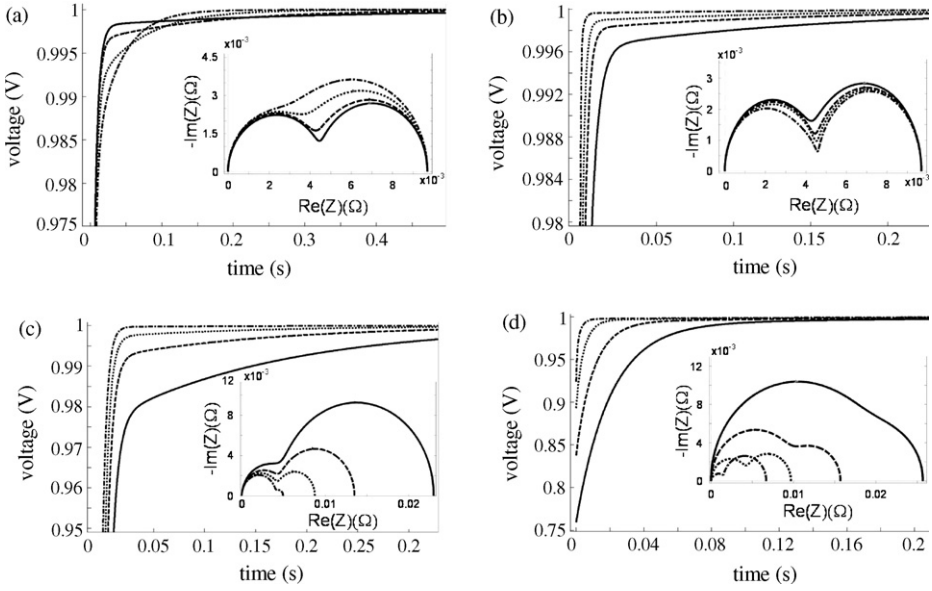

Fig. 6. Simulated cell voltage after CI and impedance spectra for selected parameter values. Baseline: $\tau_d = 0.5$ s, $C_{dl} = 0.1$ F, $R_d = 6$ mΩ and $R_p = 4$ mΩ. (a) τ_d ={1 s (—), baseline (––), 0.2 s (· · ·), 0.1 s (–·–)}; (b) C_{dl} ={baseline (—), 0.5 F (––), 0.2 F (· · ·), 0.1 F (–·–)}; (c) R_d ={20 mΩ (—), 10 mΩ (––), baseline (· · ·), 1 mΩ (–·–)}; and (d) R_p ={20 mΩ (—), 10 mΩ (––), baseline (· · ·), 1 mΩ (–·–)}.

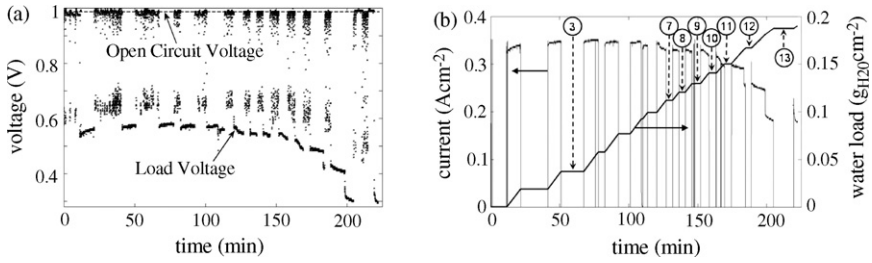

Fig. 8. Overall experiment results: (a) cell voltage and (b) cell current and estimated amount of water.

Therefore, the plant response to an interruption step can be calculated by substracting Eq. (27) from Eq. (28):

$$\sum_i k_i - \sum_i k_i(1 - \mathrm{e}^{-t/k_i\tau_i}) = \sum_i k_i\,\mathrm{e}^{-t/k_i\tau_i} \tag{29}$$

On the other hand, the plant response to a unit impulse is the following:

$$L^{-1}[F(s)] = L^{-1}\left[\sum_i \frac{k_i}{1 + k_i\tau_i s}\right] = \sum_i k_i\,\mathrm{e}^{-t/k_i\tau_i} \tag{30}$$

As Eq. (30) is equal to Eq. (29), the plant described by Eq. (26) has the same response to an interruption step than to a unit impulse.

3.8. Amount of water in the fuel cell

The amount of water ($\Delta\chi_{H_2O}$) generated by electrochemical reaction in the fuel cell during the time period T_m can be calculated from Eq. (31) [31]. The cell current (I_{ins}), which is supposed constant during that time period, can be calculated from the cell voltage and the load resistance (see Eq. (32)):

$$\Delta\chi_{H_2O} = \frac{C_e M_{H_2O} T_m}{S_a N_A n} I_{ins} \tag{31}$$

$$I_{ins} = \frac{V_{ins}}{R_{load}} \tag{32}$$

After N time intervals, the total amount of water in the cell, $(\chi_{H_2O})_N$, can be calculated from Eq. (33), where $(\chi_{H_2O})_0$ is the initial amount water in the cell:

$$(\chi_{H_2O})_N = (\chi_{H_2O})_0 + \sum_{i=1}^{N} (\Delta\chi_{H_2O})_i \tag{33}$$

4. Results and discussion

Cathode flooding and drying have a relevant effect on the cell performance. In order to study the effect of the cathode flooding on the cell model parameters, the parameter estimation methodology proposed in Section 3.6 can be repeatedly applied during the flooding process. The experimental set-up was described in Section 2. The data obtained from each CI experiment run, corresponding to a given cathode flooding level, is used to estimate the parameters of the cell electric model shown in Fig. 2.

The time evolution of the cell voltage and current are plotted in Fig. 8a and b, respectively. The voltage and current decrease as time passes, due to the cathode flooding.

As the cathode and the anode exhausts are closed, all the water produced by the electrochemical reaction is accumulated inside the cell. This can be used to estimate the water accumulated inside the cell (χ_{H_2O}). The initial mass of liquid water inside the cell is zero. Also, the initial cell temperature is low enough to consider that the amount of water in gas phase is negligible. The method used to estimate the water generated in the cell was discussed in Section 3.8. The time evolution of the water accumulated inside the cell is plotted in Fig. 8b.

Several CI runs are performed for different flooding conditions. The measured and fitted cell voltages for the 8th, 10th and 12th CI runs are shown in Fig. 9a. The corresponding circuit models are calculated by applying the proposed method-

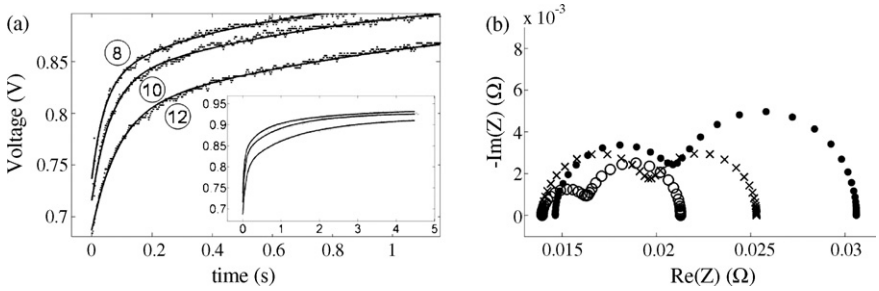

Fig. 9. Results from selected CI runs: (a) measured and fitted cell voltages obtained from 8th, 10th and 12th CI runs; and (b) impedance spectra calculated from 8th (○), 10th (×) and 12th (●) CI runs.

Table 3
PEMFC model parameters calculated for selected CI runs

CI run	C_{dl} (F)	R_d (mΩ)	R_p (mΩ)	τ_d (s)	R_m (mΩ)	χ_{H_2O} (g cm^{-2})	SSE
3rd	1.006	4.63	0.50	0.271	14.6	0.037	0.68×10^{-2}
7th	0.998	5.21	1.59	0.406	13.8	0.112	0.72×10^{-2}
8th	0.994	5.62	2.01	0.463	13.9	0.120	1.01×10^{-2}
9th	0.991	5.80	3.88	0.551	10.4	0.129	1.78×10^{-2}
10th	0.989	6.35	5.30	0.779	13.9	0.141	1.03×10^{-2}
11th	0.986	8.47	5.54	0.821	12.4	0.150	1.63×10^{-2}
12th	0.984	10.8	5.71	0.874	14.6	0.167	1.06×10^{-2}
13th	0.973	18.0	6.20	0.947	17.7	0.187	1.51×10^{-2}

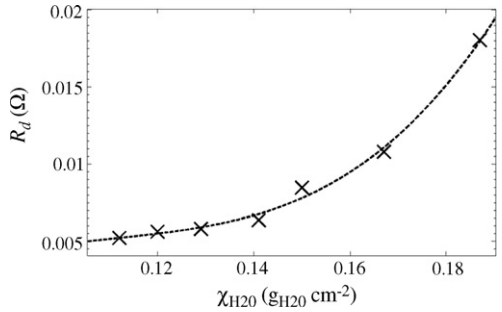

Fig. 10. Diffusion resistance (R_d) vs. accumulated amount of water (χ_{H_2O}). Calculated (×), fitted third-order polynomial (––).

ology, and they are used to obtain the impedance spectra, which are plotted in Fig. 9b. As expected [16,32], the width of the impedance arcs increases as a result of the cell flooding.

The model parameters calculated from the data of some CI runs, using the Matlab curve fitting toolbox, are shown in Table 3. The parameter SSE is the sum of the quadratic error of the curve fitting.

Note that τ_d, R_d, R_p and C_{dl} depend on the amount of water accumulated inside the cell (χ_{H_2O}). In particular, the diffusion resistance (R_d) depends on the diffusion media coefficient and the oxygen concentration on the active surface (see Eq. (3)). The relationship between R_d and χ_{H_2O} is plotted in Fig.. The points calculated from the 7th, 8th, 9th, 10th, 11th, 12th and 13th CI runs are represented by the symbol ×. The third-order polynomial fitted to these points is the following:

$$R_d = 25\chi_{H_2O}^3 - 8.3\chi_{H_2O}^2 + 0.96\chi_{H_2O} - 0.033 \quad (34)$$

5. Conclusions

A PEMFC circuit model, well suited for control applications, and a methodology for model parameter estimation from CI data, have been proposed. A key advantage of this approach is that the equipment required to perform the CI tests is easily portable and inexpensive. As a consequence, it can be implemented in cell commercial systems for in-field assessment of the cell. The proposed modelling methodology has been successfully applied to the study of the cathode flooding phenomenon.

Acknowledgements

This work has been supported by the Spanish CICYT, under DPI2004-01804 grant, and by the IV PRICIT (Plan Regional de Ciencia y Tecnologia de la Comunidad de Madrid, 2005–2008), under S-0505/DPI/0391 grant.

References

[1] D.M. Bernardi, M.W. Verbrugge, J. Electrochem. Soc. 139 (1992) 2477–2491.
[2] K. Broka, P. Ekdunge, J. Appl. Electrochem. 27 (1997).
[3] V. Gurau, H. Liu, S. Kakac, AIChE J. 44 (1998) 2410–2422.
[4] A. Rowe, X. Li, J. Power Sources 102 (2001) 82–96.
[5] J.S. Yi, T.V. Nguyen, J. Electrochem. Soc. 145 (1998) 1149–1159.
[6] S. Um, C.Y. Wang, J. Power Sources 125 (2004) 40–51.
[7] T. Zhou, H. Liu, J. Power Sources 138 (2004) 101–110.
[8] D. Bevers, M. Wöhr, K. Yasuda, K. Oguro, J. Appl. Electrochem. 27 (1997).
[9] M. Ceraolo, C. Miulli, A. Pozio, J. Power Sources 113 (2003) 131–144.
[10] B.R. Silversen, N. Djalali, J. Power Sources 141 (2005) 65–78.
[11] T.E. Springer, M.S. Wilson, J. Electrochem. Soc. 140 (1993) 3513–3526.
[12] N. Wagner, J. Appl. Electrochem. 32 (2002) 859–863.
[13] M. Ciureanu, H. Wang, J. Electrochem. Soc. 146 (11) (1999) 4031–4040.
[14] B. Andreaus, A.J. McEvoy, G.G. Scherer, Electrochem. Acta 47 (2002) 2223–2229.
[15] X. Yuan, J.C. Sun, M. Blanco, H. Wang, J. Zhang, D.P. Wilkinson, J. Power Sources 161 (2006) 920–928.
[16] N. Fouquet, C. Doulet, C. Nouillant, G. Dauphin-Tauguy, B. Ould-Bouamama, J. Power Sources 159 (2005) 905–913.
[17] T.E. Springer, Rainstrick, J. Electrochem. Soc. 136 (1989) 1594–1603.
[18] J.R. Macdonald, Impedance Spectroscopy, John Wiley & Sons, Canada, 1987.
[19] A.G. Hombrados, L. Gonzalez, M.A. Rubio, W. Agila, E. Villanueva, D. Guinea, E. Chimarro, D. Moreno, J.R. Jurado, J. Power Sources 151 (2005) 25–31.
[20] M. Boillot, C. Bonnet, N. Jatroudakis, P. Carre, S. Didierjean, F. Lapicque, Fuel Cells 1 (2006) 31–37.
[21] J. Larminie, A. Dicks, Fuel Cell System Explained, John Wiley & Sons, England, 2000.
[22] M. Usman Iftikhar, D. Riu, F. Druart, S. Rosini, Y. Bultel, N. Retiere, J. Power Sources 160 (2006) 1170–1182.
[23] J.N. Juang, Applied System Identification, PTR Prentice-Hall, New Jersey, 1994.
[24] J.P. Norton, An Introduction of Identification, Academy Press, London, 1986.
[25] K. Ogata, Ingeniería de Control Moderno, Prentice-Hall Hispanoamericana, Mexico, 1985.
[26] R.F. Mann, J.C. Amphlett, M.A.I. Hooper, H.M. Jensen, B.A. Peppley, P.R. Roberge, J. Power Sources 86 (2000) 173–180.
[27] D. Natarajan, T.V. Nguyen, J. Electrochem. Soc. 148 (2001) 1324–1335.

[28] L. Pisani, G. Murgia, M. Valentini, B. D'Aguanno, J. Power Sources 108 (2002) 192–203.
[29] I. Sadli, P. Thounthong, J.-P. Martin, S. Raël, B. Davat, J. Power Sources 156 (2006) 119–125.
[30] T. Mennola, M. Mikkola, M. Noponen, T. Hottinen, P. Lund, J. Power Sources 112 (2002) 261–272.
[31] M.A. Rubio, W. Agila, A.G. Hombrados, L. Gonzalez, E. Villanueva, J.R. Jurado, D. Guinea, Proceedings of the XVIII Eurosensors, Rome, 2004.
[32] W. Merida, D.A. Harrington, J.M. Le Canut, G. McLean, J. Power Sources 161 (2006) 264–274.